Journal of the European Ceramic Society 20 (2000) 1837–1844

CVD-coated boron nitride on continuous silicon carbide fibres: structure and nanocomposition

E. Pippel [a,*], J. Woltersdorf [a], D. Dietrich [b], S. Stöckel [b], K. Weise [b], G. Marx [b]

[a] *Max-Planck-Institut für Mikrostrukturphysik, Weinberg 2, D-06120 Halle, Germany*
[b] *Technische Universität Chemnitz, Physikalische Chemie, D-09107 Chemnitz, Germany*

Received 13 October 1999; received in revised form 10 February 2000; accepted 15 February 2000

Abstract

Boron nitride is isoelectronic with graphite, has a similar bonding structure, but a stronger localization of the π-states, and a better oxidation resistance. Therefore, it is a promising alternative to pyrolytic carbon as a tool for tayloring special fibre/matrix interlayers in composites for gas turbine and aircraft applications. To understand the CVD processing via a boron-organic precursor and to improve the thermomechanical and hydrolytic stability of the BN fibre coatings, we focussed our investigations on the question: "In what way do carbon and oxygen become incorporated into the BN layer?" HREM studies showed the turbostratic structure of the BN, forming cells of 5–10 nm in diameter. Energy filtered electron microscopy (EFTEM) and the nanometre resolved analysis of the electron energy-loss near edge structure (ELNES) of the individual elements revealed a correlation between microstructure and chemical composition. There is a general deficiency of 10–15% of nitrogen with respect to boron, which is partly compensated for by contents of up to 10 and 15% of oxygen and carbon, respectively, in the layer. It could be concluded that most of the carbon is precipitated in between the BN cells, and a smaller amount is incorporated within the hexagonal BN structure.

Zusammenfassung

Bornitrid ist isoelektronisch mit Graphit und hat eine ähnliche Bindungsstruktur. Seine π-Zustände sind jedoch stärker lokalisiert, und es weist eine bessere Oxidationsbeständigkeit auf. Aus diesen Gründen stellt BN eine vielversprechende Alternative zu pyrolytischem Kohlenstoff bei der Optimierung spezieller Faser/Matrix Grenzschichten in Verbundwerkstoffen für Gasturbinen und Flugzeugkonstruktionen dar. Um den CVD-Prozeß mittels bororganischen Precursoren sowie die thermomechanische und hydrolytische Stabilität von BN-beschichteten Fasern zu verstehen, wurde untersucht, auf welche Weise Kohlenstoff und Sauerstoff in die BN-Beschichtung eingebaut werden. HREM-Untersuchungen wiesen die turbostratische Struktur des BN mit Zellenbildung von 5–10 nm Durchmesser nach. Energiegefilterte Elektronenmikroskopie (EFTEM) und Analyse der kantennahen Elektronenenergieverlust-Feinstruktur (ELNES) ermöglichten eine Korrelation zwischen Struktur und chemischer Zusammensetzung im Nanometerbereich. In der Schicht wurde ein 10–15%iger Defizit an Stickstoff gefunden, der teilweise durch ≈10% Sauerstoff und bis zu 15% Kohlenstoff kompensiert wird. Der größte Teil des Kohlenstoffs wird zwischen den BN-Zellen ausgeschieden, ein geringer Teil ist in das hexagonale BN-Gitter eingebaut.

Keywords: BN; Composites; CVD; Electron microscopy; SiC fibres

1. Introduction

The application of long-fibre reinforced ceramic matrix composites in modern gas turbine or aircraft applications is mainly based on the outstanding properties of these composites, e.g. high-temperature resistance and an appreciable toughness. To fulfil their reinforcing role, in general, the fibres have to be coated with a thin layer of another material for mechanical, thermal, and chemical adaptation.[1] Sometimes, a suitable interlayer can be formed by transport or exchange reactions during the production of the composite material.[2]

Special coatings can act as diffusion barriers to prevent degrading fibre/matrix reactions in the subsequent processing or as sliding layers to provide the desired

* Corresponding author. Fax: +49-345-5511223.

0955-2219/00/$ - see front matter
PII: S0955-2219(00)00062-5

degree of bonding between fibre and matrix in order to optimize the mechanical properties of the composite materials.[3,4] In this respect, thin carbon layers deposited on the fibres prior to the matrix infiltration have been frequently used.[5,6] Unfortunately, the high-temperature lifetime of composite materials with a pyrocarbon interphase is strongly limited by the low oxidation resistance of carbon. Recently, boron nitride, which is isoelectronic with graphite and has a similar bonding structure, but a stronger localization of the π-states, has been proposed as a more promising alternative to pyrocarbon because of its graphite-like texture, allowing the required fibre/matrix sliding, and its better oxidation resistance.[7–10]

Actually, the BN layers should have a low impurity content, as oxygen, for example, lowers the temperature stability by the sublimation of boron oxide. On the other hand, a small amount of oxygen as well as carbon impurities incorporated into the boron nitride lattice seem to enhance its stability to hydrolysis.[26] In a previous study,[12,13] transmission electron microscopy (TEM) yielded some valuable information concerning the microstructure of boron nitride layers chemical vapour deposited (CVD) on different ceramic fibres, including details on the film thickness, its uniformity, crystal dimensions, and the quality of the fibre/BN interface. Information on the chemical composition of the BN layer has been gained via photoelectron spectroscopy (XPS)[13] and secondary ion mass spectroscopy (SIMS),[15] which confirmed the layer to consist of nearly stoichiometric BN with some excess of boron and 5–10 at% oxygen and carbon, respectively. Unfortunately, due to the special geometry of the multi-filament samples the depth resolution of the obtained composition profiles is strongly limited. Further uncertainties arise from the sputtering procedure used in the above methods being an integral one and therefore not allowing a determination of the local structure/chemistry correlation at the individual fibres. Moreover, a contribution of the specimen mount and of the interior of possibly broken fibres to the measuring signal cannot be excluded.

To overcome these difficulties and to get a more spatial-resolved chemical analysis down to the nanometre range, the present paper describes results obtained by employing high resolution transmission electron microscopy (HREM), electron energy-loss spectroscopy (EELS) in the nanoprobe mode, and electron energy filtered transmission electron microscopy (EFTEM). The latter relatively new method enables the imaging with inelastically scattered electrons of a certain energy range. The combination with an appropriate computer equipment allows the sensitive mapping of a specific element at a high spatial resolution (<1 nm) within a few seconds so that a structure/chemistry relation is easy to obtain.

The studies have been performed on CVD boron nitride layers on SiC-Nicalon® fibres. Besides microstructure and nanocomposition, particular emphasis has been placed on the question in which way do carbon and oxygen become incorporated into the BN layer. Respective results have been gained from EFTEM and the analysis of the electron energy-loss near edge structure (ELNES) of the individual elements.

2. Experimental

The Nicalon® NL 202 fibres have been coated with BN via a conventional isothermal CVD process in a hot wall reactor at 1100°C under atmospheric pressure. Details of the coating process and a schematic representation of the reactor are given in.[11,16] Prior to coating, the continuous fibres were thermally desized in an argon atmosphere (purity 99.996%) at 900°C for 2 min. As the reaction gas, a mixture of ammonia and a proprietary boron-organic precursor has been used. To have an almost stoichiometric BN layer, which is resistant to both oxygen and moisture, ammonia has been added in excess (nitrogen to boron ratio: $N/B = 100$).

For electron microscope investigations, thin specimens were prepared by standard techniques, i.e. gluing the coated fibres between ceramic dummies, cutting thin (<200 μm) slices, dimple-grinding to about 10 μm, and final Ar-ion milling (Gatan Duo-Mill) down to electron transparency. This enabled the high resolution and energy filtered imaging of specimens of only a few nanometres in thickness and a tolerable surface roughness.

Microstructure investigations followed using the high resolution Philips CM 20 FEG field emission electron microscope, run at 200 kV and equipped with a Gatan Imaging Filter (GIF 200), mounted below the microscope column. Besides electron energy loss spectroscopy at an energy resolution of 0.8–1 eV, this filter enables the element or chemical-bond specific imaging (EFTEM). The filtered images were digitally recorded by a slow-scan CCD camera within the GIF. Further details concerning the proper operation conditions of the GIF equipment are given in Ref. 17. For the image processing and the EEL spectrum treatment the Gatan Digital Micrograph was used as well as the ELP software, loaded on a Power Macintosh 7200/75.

3. Results and discussion

3.1. Microstructure and composition

At medium magnifications, the TEM image of Fig. 1 demonstrates the almost even and uniform development of the BN layer (middle part) 270 nm (±5%) thick in

this case. A preparation- induced cracking or separation between fibre and layer has not been observed, indicating a tight bonding between both.

The HREM images (cf. Fig. 2) clearly reveal the turbostratic structure of the BN layer with a spacing of 0.367 nm of the (002) BN hexagonal basic lattice planes. The observed high structural perfection of the stacking sequence of the aromatic BN planes is limited to small volumes forming nanocrystals or a cellular structure of only some nanometres in diameter. Similar results have been obtained for the BN coated carbon and alumina fibres,[12,13] for example, thus, being inherent in the BN crystal structure resembling that of graphite as mentioned above.

For a qualitative overall impression of the chemical composition of the BN coated fibres energy filtered elemental maps (EFTEM) have been made of cross-sections at medium magnification yielding a two-dimensional element distribution. The EFTEM method is based on the spectroscopy of inelastically scattered electrons: First, an energy window ($\Delta E = 10...30$ eV) is inserted in the imaging filter (GIF) behind the characteristic energy loss edge of interest in the EEL spectrum. With the selected electrons, a subsequent electron-optical system forms an image, which is digitized by a slow scan CCD camera. Because of the low specific signal in the EEL spectrum the background has to be removed by recording one or two additional images using the same energy window in positions directly in front of the edge onset. The calculation of an element specific image is now possible by dividing the image behind the ionization edge by one image in front of it (ratio map), or by subtracting the background, modelled with the two pre-edge images based on an exponential law, from the post-edge image (elemental map). While the latter method results in a true element distribution the former leads to an improved signal-to-noise ratio and is only little affected by varying specimen thickness and diffraction contrast.[18] Qualitatively, both methods should yield similar results, however.

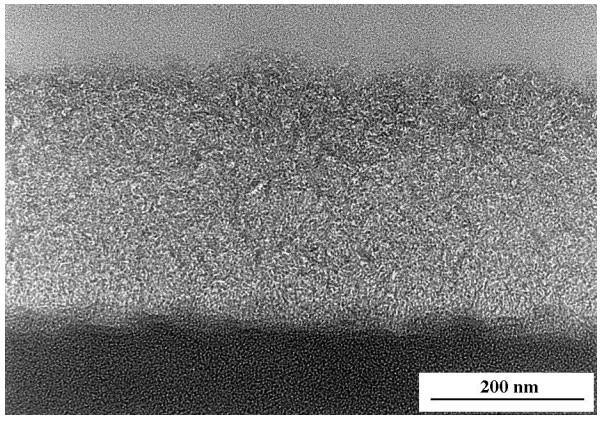

Fig. 1. TEM cross-section of a boron nitride coated (middle part) Nicalon® fibre (below).

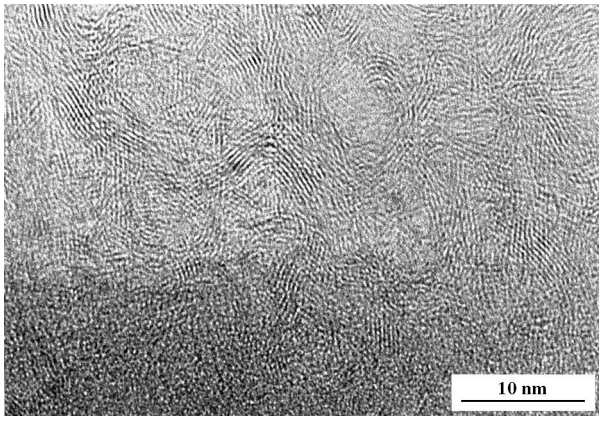

Fig. 2. High resolution image of a BN layer (upper part) on a Nicalon® fibre.

An example of an element distribution of a BN coated SiC-Nicalon® fibre is shown in Fig. 3, comprising boron, nitrogen, silicon, oxygen, and carbon. The coating mainly consists of B and N (bright contrast in Fig. 3d, e), while, as expected, Si and O occur within the fibre and, with a small quantity, in the coating, too (Fig. 3c,b). C is found in both the epoxy glue and the SiC fibre (Fig. 3f). Note that, although the images of Fig. 3 are more qualitative ones, they, nevertheless, prove the homogeneity in composition, and the relatively low interdiffusion over large areas of the system.

3.2. Quantitative element distribution

To get more detailed information on the chemical composition of the CVD BN coating, including a spatially resolved quantification in the nanometre range, EEL spectra have been recorded along a line in perpendicular orientation across the layer with interspaces of 15 nm between the spectra (probe diameter ~2 nm). The spectra comprise an energy range from 175 to 675 eV, therefore including the K-edges of the elements B (191 eV), C (283 eV), N (400 eV), and O (532 eV). Analyzing silicon has been stopped, as the exponentially increasing background in the spectrum at lower energies (Si-L23-edge: ~100 eV) would lead to intensities of 532 eV (O-K-edge) being too low to enable a proper quantification of oxygen. An example of such a set of EEL spectra is shown in Fig. 4, extending from the epoxy embedding (behind) across the BN layer to the fibre (front) in an area similar to that represented in Fig. 1. At first glance, boron and nitrogen occur only within that layer with some amount of carbon. Because of its low scattering cross section oxygen is only weakly indicated.

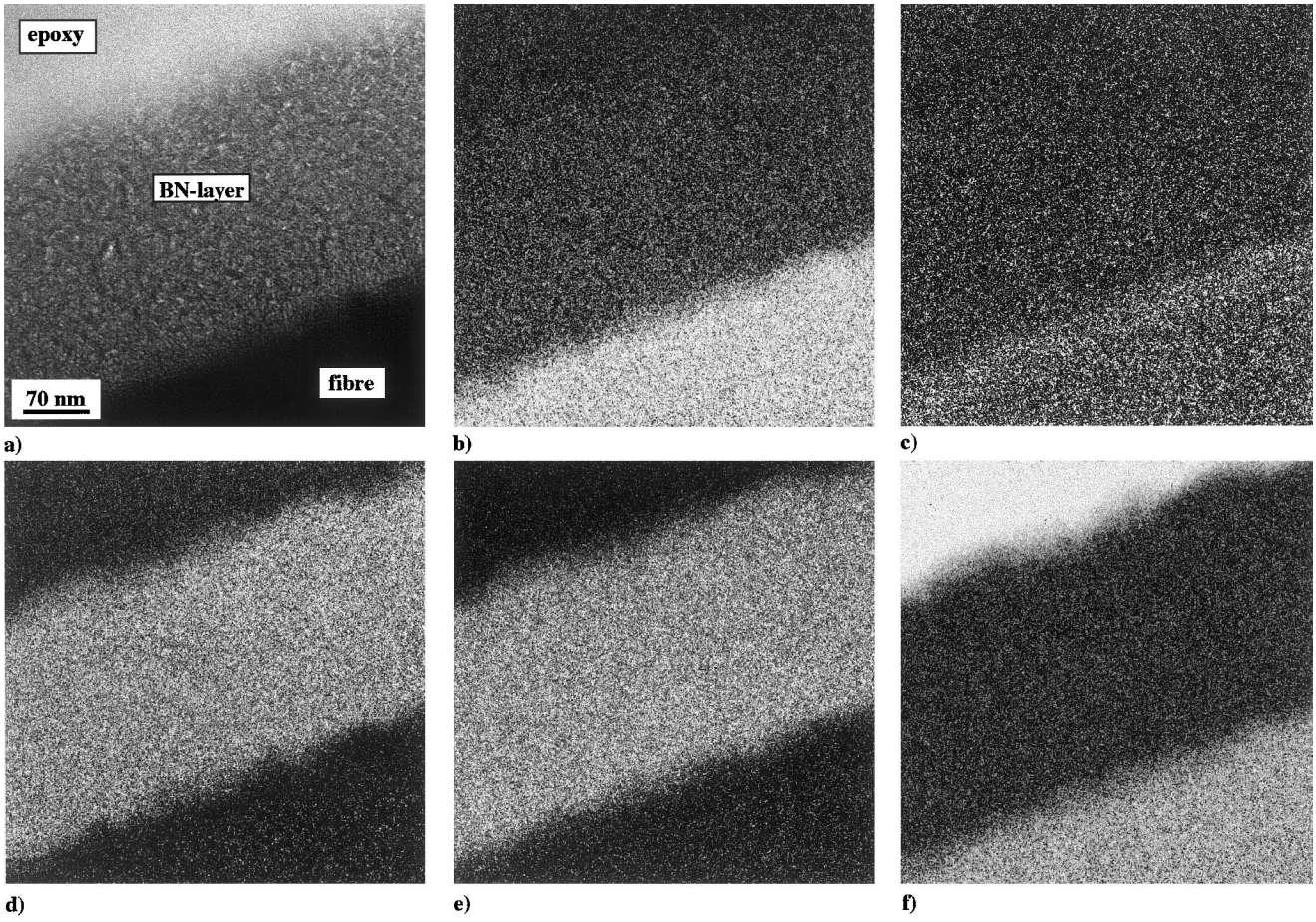

Fig. 3. (a) TEM bright-field image of a BN-coated SiC fibre (cross-section), (b)–(f) EFTEM images of Si, O, B, N, and C, respectively.

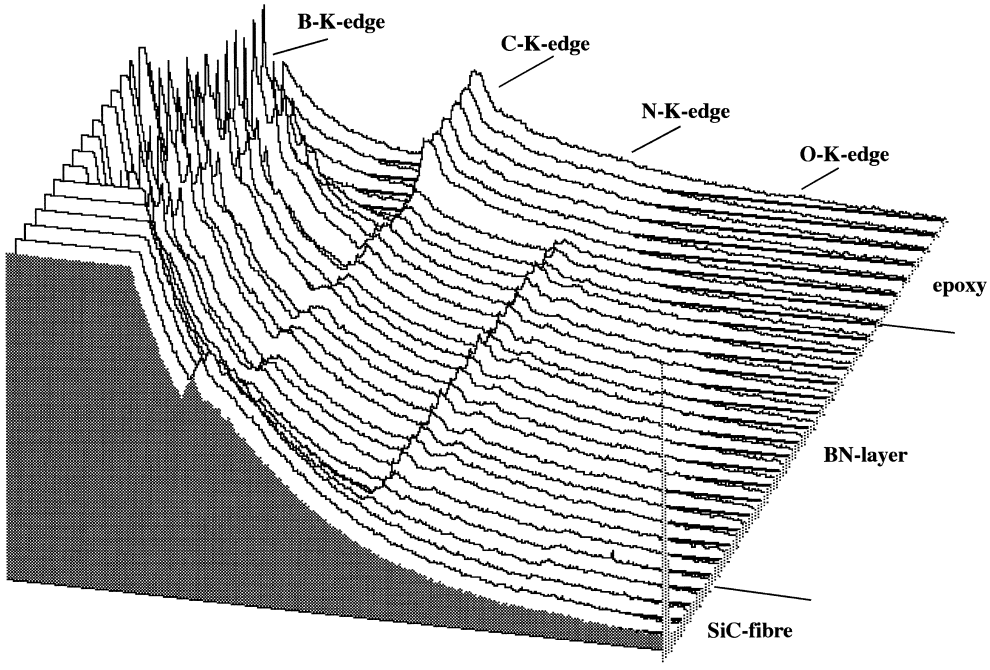

Fig. 4. Set of EEL spectra across the BN coating on a SiC fibre.

Some more information on the BN structure is obtained by interpreting the ELNES of the B and N edges, shown more clearly in the extracted spectrum of the layer in Fig. 5. Similar to the C-K edge of graphite, the B-K and N-K edges of hexagonal BN show two well separated peaks, due to the transitions of the 1s electrons into the empty π* (p_z orbitals, first peak) and σ* (p_{xy} orbitals, second peak) antibonding states, respectively.[19,20] Furthermore, as the energy of the atomic p_z orbital of nitrogen is lower than that of boron,[21] mostly, the bonding π states in BN will be filled with nitrogen p_z electrons. Accordingly, the antibonding π* states in the BN mainly consist of p_z orbitals of boron. This explains the relatively high π* resonance of the B-K edge compared to the N-K edge (cf. Fig. 5) if BN occurs in a well developed hexagonal state as shown in the HREM image of Fig. 2.

For visualizing the element distribution in the fibre/coating system the set of EEL spectra shown in Fig.4 has been quantified with respect to the elements B, C, N and O (standardless scattering cross sections, Gatan ELP-code). Fig. 6 presents the results in atom% in such a way that summing up the four elements corresponds to 100% at each measuring point. (Note that, because of the missing silicon contribution — see above — , the percentages of the other elements are overestimated in the fibre area.) According to Fig. 6a, in general, there has been a deficiency of nitrogen of 10–15% with respect to boron in the 270 nm thick coating. On the other hand, however, near the coating/fibre interface and in the upper fibre regions there is an excess of nitrogen, indicating a nitrogen diffusion into the fibre surface prior to the coating process.

Within the coating the nitrogen deficiency is almost compensated by oxygen and carbon amounting up to 10 and 15%, respectively. The fluctuations of the C and O concentrations, possibly reflect the cellular structure of the coating as shown in the high resolution image of Fig. 2. More details on the location of the impurity elements C and O will be given in Section 3.3. Finally, while the enrichment with oxygen near the surface is a typical phenomenon of Nicalon® fibres,[22] the composition gradients at the fibre/coating and coating/epoxy interfaces are attributed to the surface roughness and the overlapping of the analyzed areas as well.

The above-described nanometre resolved EELS concentration profiles confirm distinctly similar results obtained from previous SIMS investigations.[15] Mind, however, the latter is an integral method which is based on monitoring MCs^+ molecular secondary ions including the ability to detect hydrogen. A depth calibration was derived from sputter rates determined for flat samples.[14] The SIMS profile shown in Fig. 6b has been performed on a multi-filament sample of BN coated Nicalon® fibres, exhibiting an almost stoichiometric B/N ratio and the incorporation of O, which is expectedly increasing in the layer–fibre interface (cf. above). Further impurity elements in the range below 10 at% are H and C.

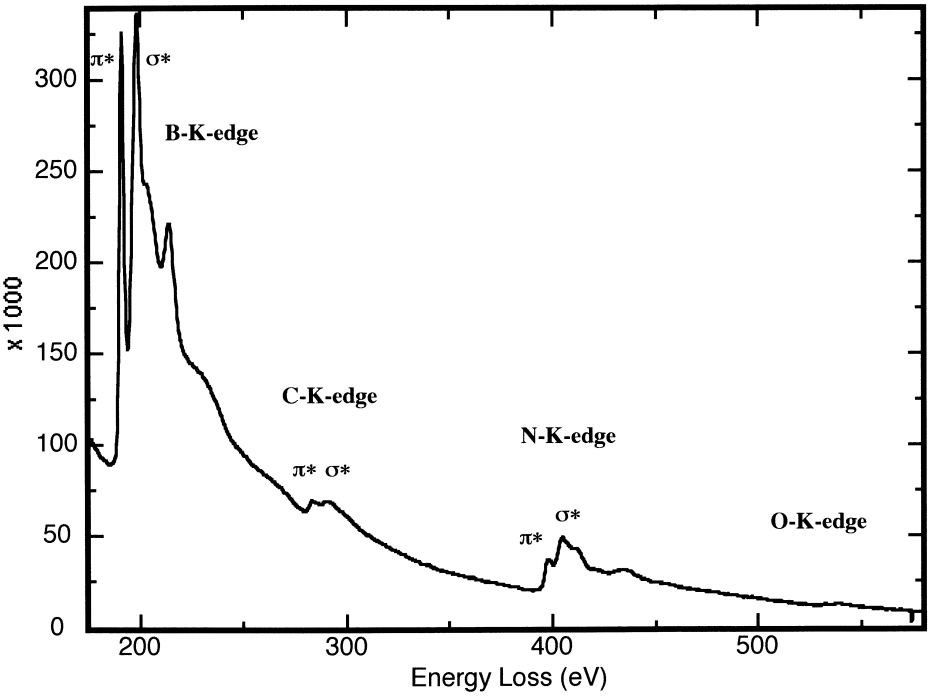

Fig. 5. Enlarged EEL spectrum from Fig. 4 (BN layer).

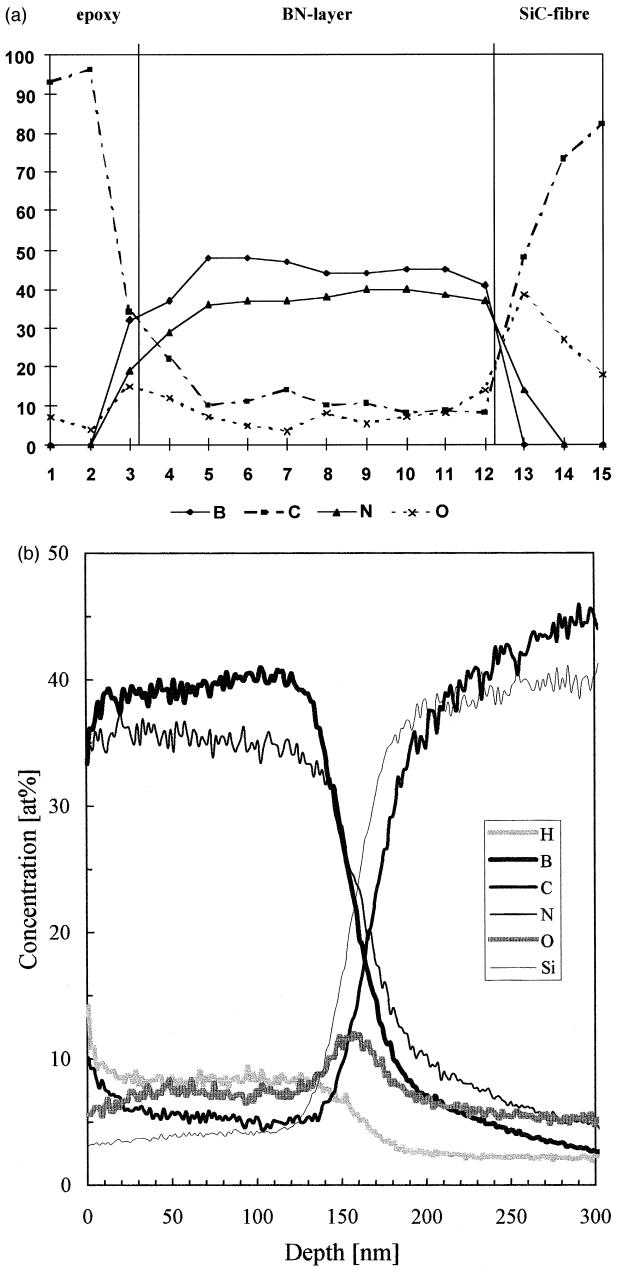

Fig. 6. (a) EELS composition profile (in at%) across a BN fibre coating; (b) SIMS composition profile (in at%) across BN coated Nicalon® fibres (fibres right).

3.3. Location of impurity elements

As mentioned in the introduction, some properties of the BN coating, such as the resistance to oxidation and hydrolysis depend on the way of incorporating the impurity elements carbon and oxygen into the layer. To elucidate the related problems, EFTEM elemental maps of the coating have been performed showing the carbon and boron distribution at an extremely high resolution. Similarly to Fig. 2, the cellular structure of the BN lamella is shown in the zero-loss filtered bright-field image of Fig. 7a. As the interspacings of the imaged (002) atomic planes of hexagonal boron and graphite differ by only ≈2%, they cannot be distinguished in the HREM image. As expected, however, the boron elemental map of the same area (see Fig. 7b) shows a high intensity in the very places of the BN atomic planes in Fig. 7a. Contrary to this, from the carbon map of Fig. 7c, it can be deduced that this element is more concentrated in regions with a lower B content and less pronounced atomic planes, located in the middle, right and at the bottom of Fig. 7a,b,c. This observation leads to the conclusion that the greater part of carbon within the BN coating has precipitated primarily in the form of nanoclusters in between the BN nano-crystals. But, nevertheless, comparing Fig. 7b and c reveals some carbon also in the BN areas possibly incorporated into the BN lattice.

To further clarify these findings the ELNES of the carbon K-edge has been investigated in detail as the intensity, energy position and width of the ELNES features as well as the threshold edge energy reflect the projected density of states in the conduction band, i.e. the electronic and crystallographic environment, and the chemical bonding state, respectively, of the element detected.[23] A typical example of the C-K-edge of carbon within the BN coating together with one of pure amorphous carbon is shown in Fig. 8. Both spectra exhibit the characteristic π^* and σ^* transitions of carbon (cf. Section 3.2). Unlike that of amorphous carbon, the π^* peak of carbon within the BN layer is somewhat higher and the σ^* peak is sharper. This hints to carbon in the coating being more graphitized[24] than that of an amorphous film. Nevertheless, the greater part of carbon within the coating should be amorphous, as can be concluded from Fig. 7.

Furthermore, the edge onset for carbon within the coating is about 2 eV lower (cf. marker line in Fig. 8). Following,[25] in a first approximation this can be interpreted to be caused by the lower binding energy of carbon incorporated into BN(C), thus being surrounded by boron atoms, the electronegativity of which is less than that of carbon. This result is consistent with the composition profile shown in Fig. 6a: In some regions of the coating, the difference of the boron and nitrogen contents cannot be compensated by oxygen, only, so that some carbon has to be incorporated to complete the BN lattice.

With respect to the location of oxygen in the BN coating layer, it was proposed recently[26] that oxygen arising from the exposure of the as-deposited BN layers to air should saturate the highly reactive dangling bonds at the borders of the turbostratic BN stacks. Because of the low signal-to-noise ratio of its EELS-K-edge and its almost uniform distribution, it has not yet been possible to image the low content of oxygen by the EFTEM technique, but respective investigations are in progress.

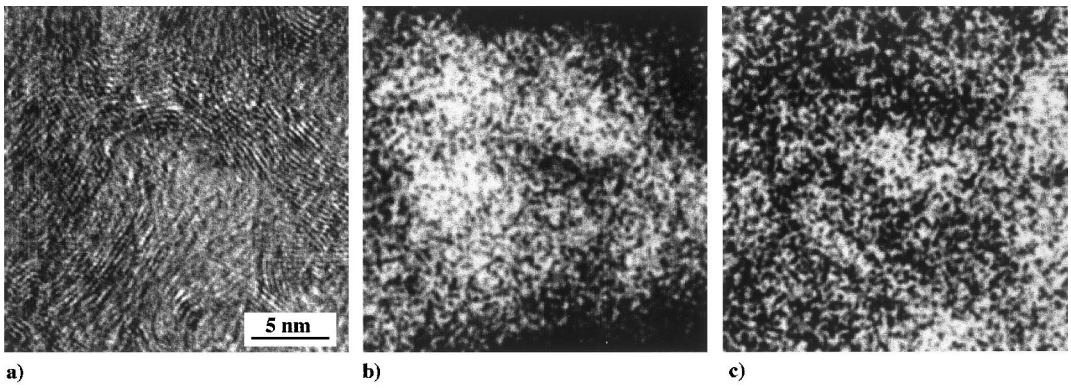

Fig. 7. (a) HREM bright-field image of a BN coating, (b) and (c) EFTEM images of boron and carbon, respectively.

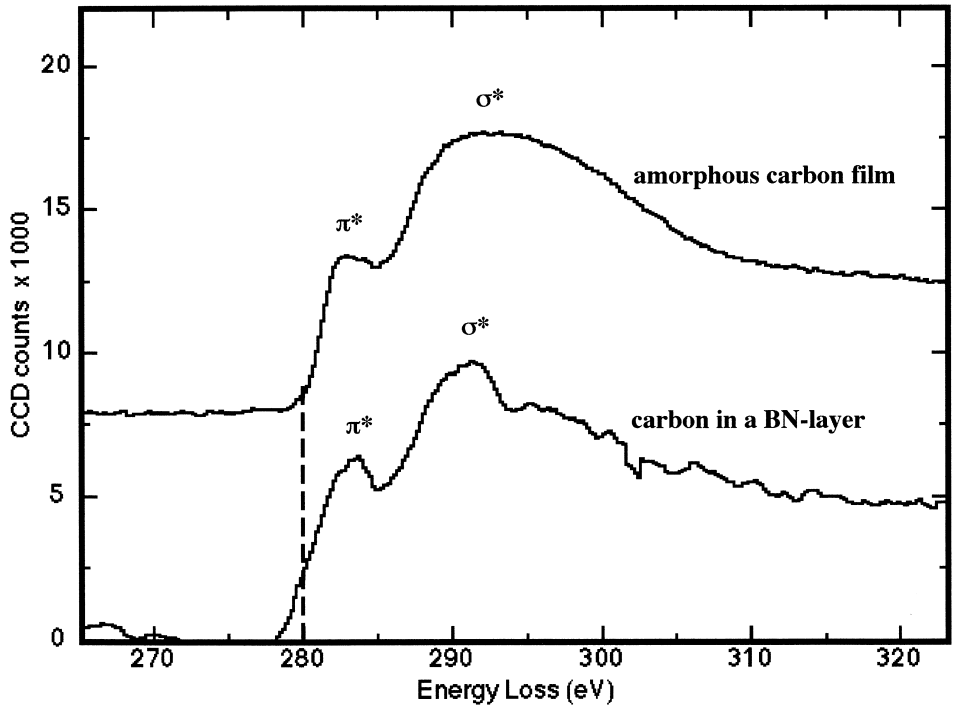

Fig. 8. ELNES of carbon K-edges.

4. Conclusions

Thin (some 100 nm) BN coatings on Nicalon® fibres have been prepared by a conventional isothermal CVD process using a boron-organic precursor in the reaction gas. HREM investigations revealed the turbostratic structure of the BN, forming cells of 5–10 nm in diameter.

The correlation of microstructure with chemical composition has been evidenced by performing nanometre resolved EELS concentration profiles across the coating. There is a general deficiency of 10–15% of nitrogen with respect to boron, which is partly compensated by contents of oxygen and carbon up to 10 and 15%, respectively, in the layer. These results confirm similar findings of previous SIMS investigations almost consistently.

Both electron energy filtered TEM images and the ELNES of C-K-edge prove that the greater part of carbon is precipitated in between the BN cells, and a smaller amount is incorporated within the hexagonal BN structure.

References

1. Feldhoff, A., Pippel, E. and Woltersdorf, J., TiN coatings in C/Mg-Al composites: microstructure, nanochemistry and function. *Phil. Mag. A*, 2000, **80**, 659–672.
2. Hähnel, A., Pippel, E., Schneider, R., Woltersdorf, J. and Suttor, D., Formation of a structure of reaction layers in SiC/glass and SiC/SiC composites. *Composites Part A*, 1996, **27A**, 685–690.
3. Pippel, E. and Woltersdorf, J., Structure, composition and function of interfaces in ceramic fibre/matrix composites. *Journal de Physique IV*, 1993, **C7**(suppl III) (3) 1905–1910.

4. Evans, A. and Marshall, D. B., The mechanical behaviour of ceramic matrix composites. *Acta metall*., 1989, **37**, 2567–2583.
5. Naslain, R., Fibre-matrix interfaces in ceramic matrix composites processed by CVI. *Composite Interfaces*, 1993, **1**, 253–286.
6. Lowden, R. A., Schwarz, O. J. and More, K. L., Improved fibre coatings for Nicalon/SiC composites. *Ceram. Eng. Sci. Proc.*, 1993, **14**, 375–384.
7. Rice, R. W., BN coatings of ceramic fibres for ceramic fibre composites. US Patent No. 4642271, 10 February 1987.
8. Singh, R. N. and Brun, M. K., Effect of boron nitride coating on fibre-matrix-interaction. *Ceram. Eng. Sci. Proc*., 1987, **8**(7–8), 636–643.
9. Gonczy, S. T., Butler, E. P., Khasgiwale, N. R., Tsakalakos, L., Cannon, W. R. and Danforth, S. C., Blackglas-Nicalon composites with CVD BN fibre interface coatings. *Ceram. Eng. Sci. Proc*., 1995, **16**(4), 433–441.
10. Lowden, R. A. and More, K. L., The effect of fibre coatings on interfacial shear strength and the mechanical behaviour of ceramic composites. *Mater. Res. Soc. Proc*., 1990, **170**, 205–214.
11. Weise, K., Stöckel, S. and Marx, G., Hydrolysestabilität von CVD-BN-Schichten auf Endlosfasern für keramische Verbundwerkstoffe. In *Werkstoffwoche '98 Band IX, Symp. 11*, Hrsg. H. Dimigen, W. Paatsch, Wiley-VCH, 1999, pp. 121–126.
12. Dietrich, D., Martin, P. W., Nestler, K., Stöckel, S., Weise, K. and Marx, G., Transmission electron microscopic investigations on SiC- and BN-coated carbon fibres. *J. Mater. Sci*., 1996, **31**, 5979–5984.
13. Dietrich, D., Stöckel, S., Weise, K., Nestler, K. and Marx, G., Characterization of boron nitride fibre coatings with different crystalline order by TEM and XPS. *Fresenius J. Anal. Chem*., in press.
14. Willich, P. and Wischmann, U., Quantitative analysis of BN(C,O,Ar,H)-coatings using EPMA and SIMS. *Mikrochim. Acta* 1998, **15**(Suppl.), 141–147.
15. Dietrich, D., Willich, P., Stöckel, S., Weise, K. and Marx, G., SIMS profiling and TEM of CVD films on multi-filament samples. *Mikrochim. Acta*, submitted.
16. Hinke, S., Stöckel, S. and Marx, G., Characterization of BN-films deposited onto carbon fibres by a continuous CVD-process. *Fresenius J. Anal. Chem*., 1994, **349**, 181.
17. Krivanek, O. L., Grubbens, A. J., Dellby, N. and Meyer, C. E., Design and first application of a post-column filter. *Micr. Microanal. Microstruct*., 1992, **3**, 187–199.
18. Hofer, F., Warbichler, P. and Grogger, W., Imaging of nanometer-sized precipitates in solids by electron spectroscopic imaging. *Ultramicroscopy*, 1995, **59**, 15–31.
19. Jaouen, M., Hug, G., Gomet, V., Demazeau, G. and Tourillon, G., An EELS and XAS study of cubic boron nitride synthesized under high pressure-high temperature conditions. *Micosc. Microanal. Microstruct*., 1995, **6**, 127–139.
20. Ma, H., Lin, S. H., Carpenter, R. W., Rice, P. and Sankey, O. F., Ab initio calculation of band structure, x-ray emission, quantum yield, and electron-energy-loss spectra of hexagonal boron nitride. *J. Appl. Phys*., 1993, **73**(11), 7422–7426.
21. Terauchi, M., Tanaka, M. and Saito, Y., Electron energy-loss spectroscopy study of the electronic structure of boron nitride nanotubes. *J Electr. Microscopy*, 1998, **47**(4), 319–324.
22. Schneider, R., Woltersdorf, J. and Röder, A., EELS nanoanalysis for investigating both chemical composition and bonding of interlayers in composites. *Mikrochimica Acta*, 1997, **125**, 361–365.
23. Brydson, R., Probing the local structure and bonding at interfaces and defects using EELS in the TEM. *J. of Microscopy*, 1995, **180**, 238–249.
24. Egerton, R. F. (ed.), *Electron Energy-Loss Spectroscopy in the Electron Microscope*. Plenum Press, New York, 1996, p. 364.
25. Kawaguchi, M., B/C/N materials based on the graphite network. *Adv. Mater*., 1997, **9**, 615–625.
26. Dietrich, D., Stöckel, S. and Marx, G., XPS investigations on boron nitride fibre coatings prepared by chemical vapour deposition in comparison to their hydrolytic rate. *Fresenius J. Anal. Chem*., 1998, **361**, 653–655.